Journal of Applied Physics

RESEARCH ARTICLE | JUNE 18 2010

Biaxial strain-induced suppression of spinodal decomposition in GaMnAs and GaCrAs

Clóvis Caetano; Lara Kühl Teles; Marcelo Marques; Luiz G. Ferreira

J. Appl. Phys. 107, 123904 (2010)
https://doi.org/10.1063/1.3448025

Biaxial strain-induced suppression of spinodal decomposition in GaMnAs and GaCrAs

Clóvis Caetano,[1,2] Lara Kühl Teles,[1,a)] Marcelo Marques,[1] and Luiz G. Ferreira[3]
[1]*Instituto Tecnológico de Aeronáutica, São José dos Campos, São Paulo 12228-900, Brazil*
[2]*Universidade Federal da Fronteira Sul, 85770-000 Realeza, PR, Brazil*
[3]*Instituto de Física, Universidade de São Paulo, CP 66318, 05315-970 São Paulo, SP, Brazil*

(Received 19 February 2010; accepted 14 May 2010; published online 18 June 2010)

The thermodynamic properties of the magnetic semiconductors GaMnAs and GaCrAs are studied under biaxial strain. The calculations are based on the projector augmented wave method combined with the generalized quasichemical approach to treat the disorder and composition effects. Considering the influence of biaxial strain, we find a tendency to the suppression of binodal decomposition mainly for GaMnAs under compressive strain. For a substrate with a lattice constant 5% smaller than the one of GaAs, for GaMnAs, the solubility limit increases up to 40%. Thus, the strain can be a useful tool for tailoring magnetic semiconductors to the formation or not of embedded nanoclusters. © *2010 American Institute of Physics*. [doi:10.1063/1.3448025]

I. INTRODUCTION

Considerable research activities have been directed toward the development of functional magnetic semiconductors (MS), formed by alloying transition metal (TM) atoms in conventional semiconductors, due to their potential application on spintronics.[1] The great advantage of MS is to allow an interplay between magnetic and electronic properties, being structurally compatible with most semiconductors epitaxially grown, which also make them potential materials for integration of photonic, electronic, and magnetic devices on a single chip.

Nevertheless, one well-known difficulty in the development of functional MS is the limited solubility of TMs in semiconductors, which rarely exceeds a few percent, except for Mn in II-VI compounds. It is already known that these materials show a tendency to spinodal decomposition, leading to second phases and TM-rich regions, as observed experimentally[2–4] and predicted theoretically.[2,5–8] Spinodal decomposition occurs below a critical temperature and for a range of the alloy composition which defines a miscibility gap at a given temperature. Although spinodal decomposition offers the possibility to have high Curie temperature in MS,[9] opening doors for potential applications, such second phases can greatly affect the electronic properties of the material.[10] Moreover, the electrical conductivity competition between half-metallic, semiconducting, or metallic character sensitively depends on concentration and dopant distribution.[11]

To overcome the formation of these embedded nanoclusters, several methods have been proposed. One of them is the digital δ-doping perpendicular to the growth direction for nitride systems.[11,12] Another possible mechanism is the codoping of DMS with shallow acceptors or donors, which could provide a means for precluding or promoting the ion aggregation during epitaxy.[10,13,14] It was also reported that the hydrostatic pressure can have some influence on the phase stability.[15] On the other hand, it has been recognized from theory and experience for a long time that the critical temperature lowers significantly due to biaxial strain in coherently grown semiconductor epitaxial layers and the miscibility gap may even be suppressed.[16,17] However, for MS only few works studied and/or analyzed the stability and its relation with external biaxial strain.[7,18] Therefore, a deep understanding of the role played by strain on phase separation in GaMnAs and GaCrAs layers is highly desirable.

It is also worth pointing out that even for the situations in which the phase separation can lead to important technological application[19] the role of the influence of strain on the phase diagram is an important study, since the composition of these second phases can change if the phase diagram changes,[20] which means that if there is some influence of the strain on the spinodal decomposition it will also have some influence on these embedded nanoclusters.

In this paper, we present a systematic theoretical study of the effect of biaxial strain on GaMnAs and GaCrAs. We show that external biaxial strain can diminish spinodal phase separation in thin GaMnAs and GaCrAs epitaxial layers pseudomorphically grown on thick unstrained zincblende *zb* (001) buffer layers or substrates, as we will name here after. We studied the influence of the biaxial strain considering several fictitious substrates with different lattice constants a_S, taking the lattice constant of GaAs as reference, we considered $0.95a_{\mathrm{GaAs}} < a_S < 1.05a_{\mathrm{GaAs}}$.

II. COMPUTATIONAL DETAILS

The calculations are based on first-principles methods combined with the generalized quasichemical approximation (GQCA), which is described elsewhere.[16,20,21] In general words, the macroscopic alloy is divided into clusters. Each cluster is realized with a certain probability. We calculated the Helmholtz free energy $F(x,T)$ which allowed us to access the $T-x$ phase diagram and obtain the critical temperature for miscibility. We express the thermodynamic potential F of the alloy as

a)Electronic mail: lkteles@ita.br.

TABLE I. All possible configurations of a distorted eight-atoms zincblende cell and their respective degeneracies, considering the total spin inversion. The numbering of atoms follows Fig. 1. The arrows indicate the directions of the local magnetic moments.

			Atomic positions			
Cluster	Configuration	Degeneracy	1	2	3	4
A	A_1	1	Ga	Ga	Ga	Ga
B	B_1	8	$Mn^{\uparrow}$	Ga	Ga	Ga
C	C_1	4	$Mn^{\uparrow}$	$Mn^{\uparrow}$	Ga	Ga
	C_2	4	$Mn^{\uparrow}$	$Mn^{\downarrow}$	Ga	Ga
D	D_1	8	$Mn^{\uparrow}$	Ga	$Mn^{\uparrow}$	Ga
	D_2	8	$Mn^{\uparrow}$	Ga	$Mn^{\downarrow}$	Ga
E	E_1	8	$Mn^{\uparrow}$	$Mn^{\uparrow}$	$Mn^{\uparrow}$	Ga
	E_2	8	$Mn^{\uparrow}$	$Mn^{\uparrow}$	$Mn^{\downarrow}$	Ga
	E_3	16	$Mn^{\uparrow}$	$Mn^{\downarrow}$	$Mn^{\uparrow}$	Ga
F	F_1	2	$Mn^{\uparrow}$	$Mn^{\uparrow}$	$Mn^{\uparrow}$	$Mn^{\uparrow}$
	F_2	8	$Mn^{\uparrow}$	$Mn^{\uparrow}$	$Mn^{\uparrow}$	$Mn^{\downarrow}$
	F_3	2	$Mn^{\uparrow}$	$Mn^{\uparrow}$	$Mn^{\downarrow}$	$Mn^{\downarrow}$
	F_4	4	$Mn^{\uparrow}$	$Mn^{\downarrow}$	$Mn^{\uparrow}$	$Mn^{\downarrow}$

$$F(x,T) = F_0(x,T) + \Delta F(x,T), \tag{1}$$

where

$$F_0(x,T) = (1-x)F_{\mathrm{GaAs}}(T) + xF_{\mathrm{TMAs}}(T), \tag{2}$$

and

$$\Delta F(x,T) = \Delta U(x,T) - T\Delta S(x,T). \tag{3}$$

Expression (2) describes the free energy of a macroscopic mixture of the GaAs and TMAs (TM=Cr or Mn) components whose free energies are F_{GaAs} and F_{TMAs}, respectively. Expression (3) gives the mixing free energy (ΔF) as a sum of the mixing enthalpy of the alloy (ΔU) and the mixing free entropy (ΔS). The calculation of the mixing free energy was carried out by combining the cluster expansion method within the framework of the GQCA and *ab initio* density functional theory (DFT), as explained in the sequence.[22,23] The $Ga_{1-x}TM_xAs$ alloy is divided into an ensemble of clusters individually independent statistically and energetically of the surrounding atomic configuration. Each cluster j with a certain number of TM and Ga atoms is realized with a certain probability. For each cluster, we considered all possible magnetic configurations, as listed in Table I for the GaMnAs alloy. The energy of a particular cluster is taken as the average energy over its magnetic configurations, weighted by the respective degeneracies.

We used eight-atoms supercells as the basic clusters. The advantages of such cluster is described in Ref. 16. Moreover it was also shown by Osorio-Guillén *et al.*[7] for GaMnAs, that the interaction is larger for the nearest-neighbor, with the first nearest-neighbor pair interaction attractive, thus favoring the association of similar atoms, and is approximately 23 times larger than the remaining three repulsive pair interactions second, third, and fourth nearest neighbors. The three-body interactions are repulsive and their magnitudes are approximately two and six times smaller than the attractive first nearest neighbor pair interaction. The four-body interactions are all attractive and, on average, six times smaller than the first pair interaction. So the more important interactions are already included in our simulations. To model the strain influence and considering epitaxial pseudomorphic growth, we fix the in-plane lattice constants as equal to the a_S, which leads to a biaxial strain parallel to the cubic [001] direction that deforms the cubes (see Fig. 1). Consequently, the crystals consisting of a certain cluster kind become tetragonal.

As mentioned above, the total-energy and electronic-structure calculations for each cluster configuration are based on the DFT. We used the frozen-core projector-augmented wave method as implemented in the "Vienna *ab initio* simulation package" (VASP-PAW code) within a spin-polarized DFT.[24] We adopted the generalized gradient approximation for the exchange-correlation potential.[25] The lattice constant was optimized, by total energy minimization, for each configuration and the atomic positions were relaxed. It is worth pointing out that the optimization of the lattice constant and the relaxation of the atomic positions are very important, since the differences in the bond lengths result in an internal strain that, among other reasons, drives the tendency to phase

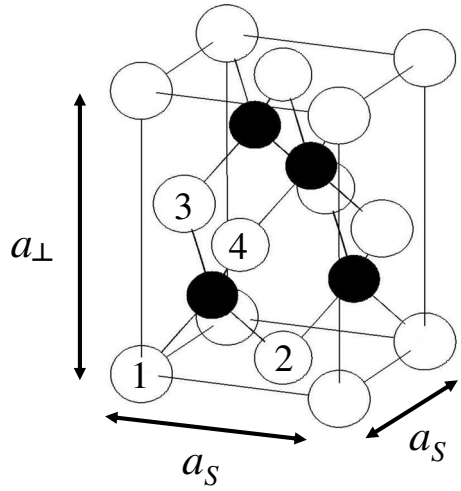

FIG. 1. Schematic representation of a cluster in a $Ga_{1-x}TM_xAs$ (TM=Cr or Mn) alloy. The empty circles represent TM or Ga atoms and the filled circles represent As atoms.

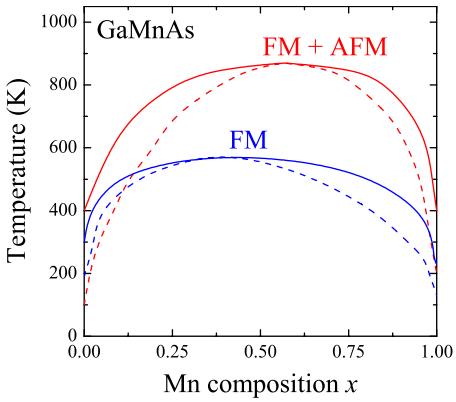

FIG. 2. (Color online) $T-x$ phase diagram for nonstrained GaMnAs considering all the configurations (red) and only the FM configurations (blue). The solid and dashed lines represent the binodal and spinodal curves, respectively.

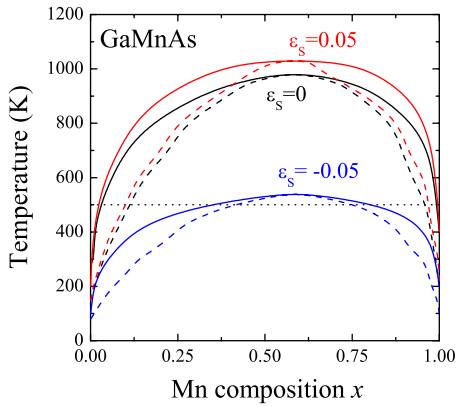

FIG. 3. (Color online) Phase diagram for strained GaMnAs, taking into account the relative difference ε_S of the fictitious substrate with respect to the GaAs lattice constant. Solid lines: binodal curves, dashed lines: spinodal curves, and dotted line: typical growth temperature

separation. Moreover, the lattice parameter of the majority of DMS does not follow the Vegard's law and depends on the composition and the magnetic moment.[26]

The $T-x$ phase diagrams were built simply by using the common-tangent method.[20] In more detail, the phase diagrams consist of the spinodal and binodal curves. The binodal curve defines the equilibrium solubility limit, i.e., the miscibility gap. In the region between spinodal and binodal curves the alloy is metastable against decomposition, and in the region inside the spinodal curve, the alloy is inherently unstable, and it defines the spinodal decomposition.[20] For temperatures and compositions above the binodal curve a homogeneous random alloy is predicted.

In agreement with the assumption that each cluster configuration j takes its own equilibrium volume, the strain $\epsilon_{j\|} = (a_\| - a_j)/a_j$ in the configuration should be different, assuming that the substrate determines (and hence fixes) the in-plane lattice constant $a_\| = a_S$ in each configuration at the same value. Consequently, a spatially different and therefore spatially inhomogeneous strain relief occurs. By taking into account that for each configuration there is a different value for $\epsilon_\|$, in order to distinguish the different cases, we define a relative difference of the lattice constant of the fictitious substrate a_S with respect to the GaAs lattice constant as

$$\varepsilon_S = \frac{a_S - a_{\mathrm{GaAs}}}{a_{\mathrm{GaAs}}}. \tag{4}$$

Thus, if $\varepsilon_S > 0$ the lattice constant of the substrate is larger than the GaAs, otherwise it is smaller.

III. RESULTS AND DISCUSSION

Before analyzing the influence of biaxial strain on the thermodynamic properties of MS alloys, we consider the simpler situation of a strain-free system. In this case, as the cubic cell is not deformed, the number of different configurations to calculate is smaller than in the general strained case. We have done two different calculations in order to build the phase diagram of GaMnAs: (i) considering only the configurations with ferromagnetic (FM) interactions and (ii) considering all the configurations, i.e., both FM and antiferromagnetic (FM+AFM) interactions. In Fig. 2 we compare the results. First of all, we note that the critical temperature in FM phase diagram (~570 K) is considerably lower than in the FM+AFM one (~870 K). Another remarkable difference concerns with the asymmetry of the phase diagrams, the alloy being more stable in the Ga rich region if we consider both FM and AFM configurations. The asymmetry in FM phase diagram is similar to the results of Nakamura *et al.*,[8] and Osorio-Guillén *et al.*[7] with Mn substitution in GaAs energetically more costly than Ga substitution in zincblende MnAs. We conclude that, even using a modest size cell and energy-average clusters, the inclusion of AFM states have an important influence on the statistical results.

Let us consider now the strained alloys. In Fig. 3, we show the phase diagrams of GaMnAs alloy for $\varepsilon_S = 0$, -0.05, and 0.05. Comparing the phase diagram for $\varepsilon_S = 0$ ($a_S = a_{\mathrm{GaAs}}$) with the phase diagram for strain-free alloy (FM+AFM in Fig. 2) we note that, for practical purposes, there is no difference in asymmetry between them, the limits of solubility being similar. The difference in critical temperatures also is not large (~100 K). Now comparing different substrate lattice parameters, we can observe that the critical temperature is high for the cases $\varepsilon_S = 0$ and $\varepsilon_S = 0.05$, and the phase diagrams are very similar, meaning that for these cases the influence of strain is negligible. In the range of growth temperatures (~500 K), we observe a phase separation for more or less the same wide range of composition. Considering, e.g., $T = 500$ K, a large decomposition tendency is seen for Mn content between 10% to 90%, which means that there is a tendency to the formation of Mn-rich nanoclusters. This result is in good agreement with experimental findings that show that samples of $Ga_{0.952}Mn_{0.048}As$ grown on InGaAs buffer layers have no significant influence of strain.[18] Also theoretical results show that, for small biaxial strain, the magnetic coupling in GaMnAs should be unaffected by strain.[27]

We show in Fig. 4 the phase diagrams for GaCrAs alloy. We can observe that the critical temperatures of GaCrAs alloy is considerably higher than of GaMnAs one. For $\varepsilon_S = 0$, e.g., the difference is about 300 K. Despite this difference in critical temperatures, for $\varepsilon_S = 0$ the limits of solubility between the two alloys are close, being 15% to 95% for GaC-

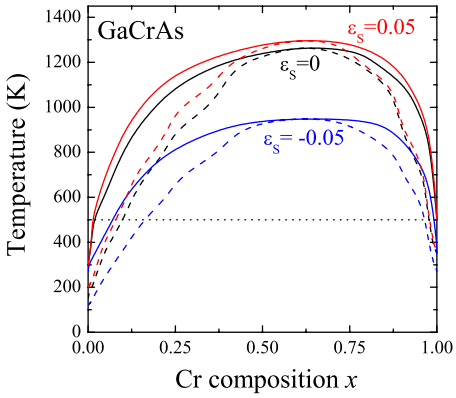

FIG. 4. (Color online) Phase diagram for strained GaCrAs, taking into account the relative difference ε_S of the fictitious substrate with respect to the GaAs lattice constant. Solid lines: binodal curves, dashed lines: spinodal curves, and dotted lines: typical growth temperature

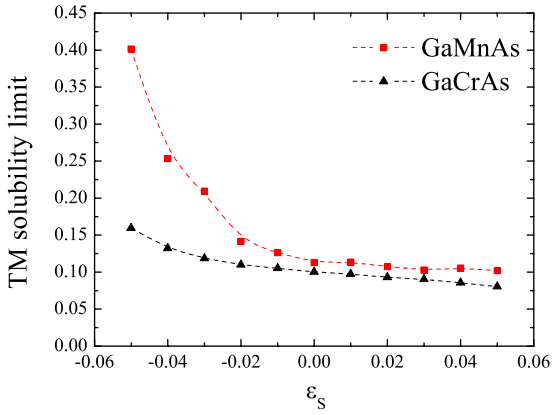

FIG. 5. (Color online) Equilibrium solubility limit of Mn and Cr on GaAs, for typical growth temperatures, as a function of the relative difference ε_S of the fictitious substrate considered in the calculation a_S with respect to the GaAs lattice constant.

rAs and, as it was shown above, 10% to 90% for GaMnAs. Again, the phase diagram of GaCrAs alloy under tensile biaxial strain ε_S=0.05 is very close to the phase diagram for ε_S=0.

However, drastic changes occur for larger compressive biaxial strains. In the case of a fictitious substrate with lattice constant 5% smaller than the GaAs, the critical temperature is reduced by about 200 K for GaMnAs and about 300 K for GaCrAs, giving now T_c(GaMnAS) ~ 600 K and T_c(GaCrAS) ~ 900 K. Simultaneously the miscibility gap as well as the region of spontaneous decomposition is reduced, in particular for smaller TM molar fractions. One can indeed speak about a tendency for suppression of the phase separation in GaTMAs due to compressive strain. The influence of strain on phase diagrams of MS was also reported by Nakamura *et al.*,[15] but only for hydrostatic strain. Furthermore, as we already pointed out before, their method considers only FM configurations for the alloy. Thus, a direct comparison between their results and ours is not possible and it is out of the scope of this paper. We must say that we do not intend to compare the effectiveness of the epitaxial strain with other possible methods, but say that it also represents one possibility to increase the solubility limit. As we are analyzing the consequences of a coherent growth of these materials on different substrates, one could argue that the critical thickness could be a problem in these systems. The overlayer initially grows in perfect registry with the substrate, however as the overlayer thickness increases, the strain energy also increases. As a result, it would eventually generate dislocations. This occurs at an overlayer thickness called the critical thickness, d_c, which is approximately given by[28]

$$d_c \cong \frac{a_S}{2|\epsilon|}, \tag{5}$$

with

$$\epsilon = \frac{a_S - a_L}{a_L}, \tag{6}$$

where a_L is the lattice constant of the overlayer. With Eqs. (5) and (6), and considering our extreme case in which a_S =0.95a_{GaAs} and a TM concentration of 40%, a rough estimate of the critical thickness results in approximately 20 monolayers. Therefore, the critical thickness is not a problem in these systems.

Next we studied in more detail the equilibrium solubility limit of Mn and Cr on GaAs as function of the substrate lattice parameter. The results are depicted in Fig. 5. We can observe that, for substrates with lattice constants 98% a_{GaAs} (ε_S=−0.02), the limit of solubility begins to increase, and the increase being more pronounced for GaMnAs than for GaCrAs. Thus we observe a tendency to a suppression of phase separation in the pseudomorphically grown alloy layers as the compressive biaxial strain increases. It is not possible to understand this behavior only by considering the strain distribution. As already stated by other authors for the unstrained case, the mismatch of the lattice parameter of zincblende GaAs and MnAs, and consequently the resulting internal strain, is not the only responsible for the phase separation process, but there is also other factors, as unfavorable chemical interactions.[29] Mahadevan *et al.*[29] studied the cluster tendencies in GaAs based MS, and obtained that the TM–TM pair interaction is stronger along [110] crystallographic direction. The authors also showed that the coupling between states with t_2 symmetry will be larger for two atoms occupying lattice positions along the zincblende bonding chain, lowering the energy of the system. This fact can explain the difference between the cases ε_S=−0.05 and ε_S =0.05, since for ε_S=−0.05 the TM atoms in the direction [110] are closer to each other than for ε_S=0.05. In the case ε_S=−0.05, the lowering of the energy of the system results in the fact that the mixing free energy begins to have a large contribution of the entropy term and the critical temperature T_c of the strained alloy decreases. Considering the difference between the solubility limit of Cr and Mn, this can be explained in terms of the tendency to cluster being stronger for GaAs doped with Cr than with Mn($T_c^{\mathrm{GaCrAs}} > T_c^{\mathrm{GaMnAs}}$). This tendency was also shown earlier by the work of Mahadevan *et al.*,[29] in which they showed that the pair and the four-body interaction energies are stronger for Cr in GaAs than for Mn in GaAs. Therefore, if one considers the same temperature, to have the same solubility limit for Cr and Mn, the strain applied in GaCrAs must be stronger than in GaMnAs.

IV. CONCLUSIONS

Summarizing, the compressive biaxial strain can be extremely important for the thermodynamic behavior of the GaMnAs and GaCrAs alloys. In general, the region of spontaneous decomposition at typical growth temperatures is reduced. In the case of GaMnAs the Mn solubility limit is significantly increased. In contrast, for tensile strain no influence was observed. This can be seen as an intriguing new insight into the properties of MS. Hopefully these studies will stimulate other experimental investigations, on other possibilities of controlling the spinodal decomposition in these materials.

ACKNOWLEDGMENTS

This work was supported by the Brazilian funding agencies CNPq and FAPESP (Grant Nos. 05/52231-0 and 06/05858-0).

[1]T. Jungwirth, J. Sinova, J. Mašek, J. Kučera, and A. H. MacDonald, Rev. Mod. Phys. **78**, 809 (2006).
[2]S. Kuroda, N. Nishizawa, K. Takita, M. Mitome, Y. Bando, K. Osuch, and T. Dietl, Nature Mater. **6**, 440 (2007).
[3]M. Moreno, A. Trampert, B. Jenichen, L. Däweritz, and K. H. Ploog, J. Appl. Phys. **92**, 4672 (2002).
[4]M. Yokoyama, H. Yamaguchi, T. Ogawa, and M. Tanaka, J. Appl. Phys. **97**, 10D317 (2005).
[5]K. Sato, H. Katayama-Yoshida, and P. H. Dederichs, Jpn. J. Appl. Phys., Part 2 **44**, L948 (2005).
[6]M. van Schilfgaarde and O. N. Mryasov, Phys. Rev. B **63**, 233205 (2001).
[7]J. Osorio-Guillén, Y.-J. Zhao, S. V. Barabash, and A. Zunger, Phys. Rev. B **74**, 035305 (2006).
[8]K. Nakamura, K. Hatano, T. Akiyama, T. Ito, and A. J. Freeman, Phys. Rev. B **75**, 205205 (2007).
[9]H. Katayama-Yoshida, K. Sato, T. Fukushima, M. Toyoda, H. Kizaki, V. A. Dinh, and P. H. Dederichs, Phys. Status Solidi A **204**, 15 (2007).
[10]T. Dietl, J. Appl. Phys. **103**, 07D111 (2008).
[11]X. Y. Cui, D. Fernandez-Hevia, B. Delley, A. J. Freeman, and C. Stampfl, J. Appl. Phys. **101**, 103917 (2007).
[12]M. Marques, L. G. Ferreira, L. K. Teles, L. M. R. Scolfaro, J. Furthmüller, and F. Bechstedt, Phys. Rev. B **73**, 224409 (2006).
[13]K. Sato and H. Katayama-Yoshida, Jpn. J. Appl. Phys., Part 2 **46**, L1120 (2007).
[14]A. Bonanni, A. Navarro-Quezada, T. Li, M. Wegscheider, Z. Matěj, V. Holý, R. T. Lechner, G. Bauer, M. Rovezzi, F. D'Acapito, M. Kiecana, M. Sawicki, and T. Dietl, Phys. Rev. Lett. **101**, 135502 (2008).
[15]K. Nakamura, T. Akiyama, and T. Ito, Appl. Surf. Sci. **254**, 7855 (2008).
[16]L. K. Teles, J. Furthmüller, L. M. R. Scolfaro, J. R. Leite, and F. Bechstedt, Phys. Rev. B **62**, 2475 (2000).
[17]A. Tabata, L. K. Teles, L. M. R. Scolfaro, J. R. Leite, A. Kharchenko, T. Frey, D. J. As, D. Schikora, K. Lischka, J. Furthmüller, and F. Bechstedt, Appl. Phys. Lett. **80**, 769 (2002).
[18]J. Daeubler, M. Glunk, W. Schoch, W. Limmer, and R. Sauer, Appl. Phys. Lett. **88**, 051904 (2006).
[19]P. N. Hai, S. Ohya1, M. Tanaka, S. E. Barnes, and S. Maekawa, Nature (London) **458**, 489 (2009).
[20]A. B. Chen and A. Sher, *Semiconductor Alloys* (Plenum, New York, 1995).
[21]C. Caetano, L. K. Teles, M. Marques, A. Dal Pino, Jr., and L. G. Ferreira, Phys. Rev. B **74**, 045215 (2006).
[22]P. Hohenberg and W. Kohn, Phys. Rev. **136**, B864 (1964).
[23]W. Kohn and L. J. Sham, Phys. Rev. **140**, A1133 (1965).
[24]G. Kresse and J. Furthmüller, Comput. Mater. Sci. **6**, 15 (1996).
[25]Y. Wang and J. P. Perdew, Phys. Rev. B **44**, 13298 (1991).
[26]C. Caetano, M. Marques, L. G. Ferreira, and L. K. Teles, Appl. Phys. Lett. **94**, 241914 (2009).
[27]T. Dietl, H. Ohno, and F. Matsukura, Phys. Rev. B **63**, 195205 (2001).
[28]J. Singh, *Electronic and Optoelectronic Properties of Semiconductor Structures* (Cambridge University Press, New York, 2003).
[29]P. Mahadevan, J. M. Osorio-Guillén, and A. Zunger, Appl. Phys. Lett. **86**, 172504 (2005).